DINAME 2023 - Proceedings of the XIX International Symposium on Dynamic Problems of Mechanics,
A.S. De Paula, A.T. Fabro and M.R. Machado (Editors), ABCM.
Pirenópolis, Go, Brazil, February 26th to March 3rd, 2023

Investigation of a rainbow metastructure for broadband vibration attenuation in a crankshaft

Nícolas da Silva Dias and Aline Souza de Paula

Universidade de Brasília, Campus Universitário Darcy Ribeiro, Faculdade de Tecnologia, Asa Norte, CEP 70.910-900, Brasília-DF

nicolassd29@gmail.com
alinedepaula@unb.br

Abstract: Torsional vibrations are usually present in rotating machines, and it is one of the leading causes of mechanical failures. This work investigates the performance of the vibration attenuation bandgap in a reciprocating compressor shaft with concentrated constant inertias attached with identical resonators and rainbow metastructures under harmonic excitation. Although the cylinder inertia has a nonlinear nature related to the shaft rotation, in the present work, to simplify the analysis and provide insightful analytical solutions, the nonlinear interactions are neglected yielding to constant inertia of the cylinder, which includes the crank-slider mechanism. Modal expansion theory is employed to obtain natural frequencies and modes including the effects of concentrated inertia. The results show that identical resonators are able to attenuate a frequency range around the target frequency. On the other hand, rainbow metastructures can produce an attenuation bandgap 600% wider than identical resonators with the same added inertia.

Keywords: torsional vibration, vibration attenuation, rainbow metastructures

INTRODUCTION

Torsional vibrations are the leading cause of failures in many rotating machines. The most common effects of uncontrolled vibrations are failed couplings, broken shafts, and worn gears, among others (Corbo and Melanoski, 1996). In general, these vibrations are caused by the excessive forces and moments that vary cyclically with periodicity given by system rotation speed (Wachel and Tison, 1994). Because of this, vibration control is a crucial subject and is widely explored by the scientific community to provide a long work life to several mechanical systems.

In the literature, the mathematical models used to describe rotating machines with crankshafts can be arranged into two main categories: linear and nonlinear. The first group considers that the inertia of the crank-rod-piston mechanism is constant. This assumption can lead to errors regarding the geometric dimensions of the equipment and operational conditions. On the other hand, Metallidis and Natsiavas (2003) and Huang *et al.* (2012) describe a better representative model by taking into account that the mechanism of inertia varies with the rotation, culminating in nonlinear equations of motion. Over the years, the influence of non-constant inertia effects has been investigated by several studies such as Pasricha and Carnegie (1976, 1979) and Brusa *et al.* (1997).

Metamaterial structures have been used extensively to attenuate vibrations in the last two decades after the pioneering works of Liu *et al.* (2000) and Sheng *et al.* (2003). This type of structure explores the coupling between local resonances and propagating waves to avoid wave transmission over frequencies near resonances. This feature was termed bandgap and it is one of the most researched interests in the literature field of vibration and acoustics control recently (Krödel *et al.*, 2015; Hu *et al.*, 2017). Vibration suppression using metamaterials was carried out with different approaches: using nonlinear metamaterial in beams, where nonlinear absorbers are attached to a linear system (Casalotti *et al.*, 2018); using rainbow metastructures that create multiple bandgaps around a target frequency (El-Borgi *et al.*, 2020); exploring nonlinear vibration attenuation through the employment of nonlinear energy sink (NES), which are lightweight single or multi-degree of freedom system responsible for mitigating energy in a one way and irreversible process directly to a cubic stiffness nonlinearity (Kani *et al.*, 2016). Several other works in the literature have proposed methods to attenuate vibrations using metastructures, such as Sugino *et al.* (2016, 2017) and Xia *et al.* (2020). Moreover, the advances in metamaterials can increase the vibration attenuation bandwidth size with lightweight periodic structures.

This work presents an analysis of the torsional vibration of a single-cylinder reciprocating compressor's crankshaft, showing the effects of the attachment of identical and rainbow metastructures in the formation of bandgaps. This paper is structured as follows. The next section describes the equations of motion of the crankshaft with the attached metastructure and its analytical solution using modal expansion theory. Then, numerical results are presented and discussed, showing the vibration attenuation of the system with identical resonators and rainbow metamaterials under a concentrated harmonic excitation. The conclusions section summarizes the main achievements of this work.

CRANKSHAFT MODEL AND RESPONSE USING MODAL COORDINATES

According to the model proposed by Metallidis and Natsiavas (2003), alternative machines are composed of two parts. The first is the compressor itself and the second represents the load. This work considers a single-cylinder reciprocating compressor, consisting of a shaft with two attached inertia, the first representing the cylinder's inertia, $I_e(\theta)$, and the latter the load's inertia I_l. Two external torques are considered, one represents the resistive torque produced by the cylinder, T_c, and the other describes the electric motor torque, T_m, as shown in Fig. 1a. The cylinder inertia is determined by using the equivalent crank-slider mechanism inertia, which is represented by Fig. 1b.

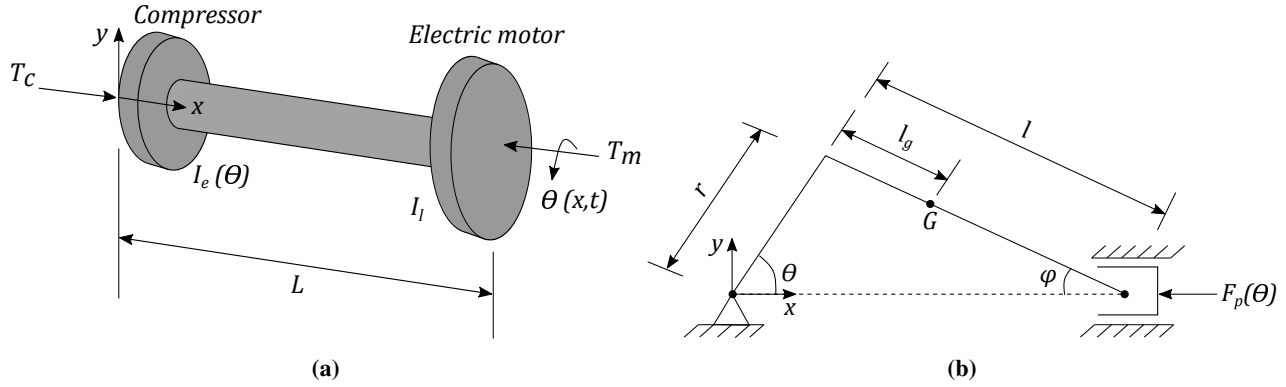

Figure 1 – Model of a single-cylinder reciprocating compressor: (a) simplified model and (b) crank-slider mechanism.

The shaft has diameter d, Elasticity's modulus E, Poisson's ratio ν, Shear's modulus $G = E/2(1+\nu)$, cross-section polar moment of inertia $J = \pi d^4/32$, density ρ, and is free to rotate at both ends ($x = 0$ and $x = L$). The governing equation of the undamped shaft, with the attached inertias, is obtained considering the torsional stiffness GJ constant and neglecting the torsional displacement of the cylinder, as follows:

$$\rho J\frac{\partial^2\theta(x,t)}{\partial t^2} + I_e(\theta)\delta(x-x_c)\frac{\partial^2\theta(x,t)}{\partial t^2} + I_l\delta(x-x_l)\frac{\partial^2\theta(x,t)}{\partial t^2} - GJ\frac{\partial^2\theta(x,t)}{\partial x^2} = T_m\delta(x-x_m) - T_c\delta(x-x_c) \qquad (1)$$

where the variable cylinder inertia, as obtained by Metallidis and Natsiavas (2003) is given by:

$$I_e(\theta) = I_c + m_1r^2 + I_2\kappa^2(\theta) + (m_2+m_p)r^2\sin^2(\theta)[1+\kappa(\theta)]^2 \qquad (2)$$

being

$$\kappa(\theta) = \frac{\lambda\cos(\theta)}{\sqrt{1-\lambda^2\sin^2(\theta)}} \qquad \text{and} \qquad \lambda = \frac{r}{l}, \qquad (3)$$

where I_c is the moment of inertia of the crank, m_p is the piston mass, m_1 is the mass of the big end, m_2 is the mass of the small end, r is the crank length, l is the total length of the connecting rod, I_2 is the additional inertia from a simplified double-mass system, $\delta(x)$ is the Dirac delta function, x_c is the cylinder position, x_l is the load position, and x_m is the electric motor position. In the present work, to simplify the analysis and provide insightful analytical solutions, the inertia is considered constant and equal to $I_e(\theta) = I_e = 0.250$ kg.m^2.

The boundary conditions of the shaft are given by:

$$\frac{\partial\theta(0,t)}{\partial x} = 0, \qquad \frac{\partial\theta(L,t)}{\partial x} = 0. \qquad (4)$$

System response can be obtained by using a modal expansion in Eq. 1 as suggested by Meirovitch (1997). The torsional displacement of the shaft is:

$$\theta(x,t) = \sum_{r=1}^{N}\eta_r(t)\phi_r(x) \qquad (5)$$

where N is the number of modes considered in the expansion and $\eta_r(t)$ is the modal weighting of the r-th mode without the concentrated inertia. The mode shapes are inertia-normalized by Eq. 7 and lead to:

$$\phi_r(x) = \sqrt{\frac{2}{\rho JL}} cos\left(\frac{(r-1)\pi}{L}x\right) \qquad r = 1,2,3,\ldots,N. \tag{6}$$

The orthonormalization conditions are satisfied as follows:

$$\int_0^L \rho J \phi_r(x)\phi_s(x)dx = \delta_{rs}, \qquad r,s = 1,2,\ldots \tag{7}$$

$$\int_0^L GJ \phi_r''(x)\phi_s(x)dx = -\omega_r^2 \delta_{rs}, \qquad r,s = 1,2,\ldots \tag{8}$$

where ω_r is the natural frequency of the r-th mode of the shaft without the concentrated inertia, and $()'$ denotes the derivative with respect to the space variable x. Introducing Eq. 5 into Eq. 1 for free torsional vibration yields in:

$$\sum_{r=1}^{N} \rho J \phi_r(x)\ddot{\eta}_r(t) + \sum_{r=1}^{N} I_e \phi_r(x)\delta(x-x_c)\ddot{\eta}_r(t) + \sum_{r=1}^{N} I_l \phi_r(x)\delta(x-x_l)\ddot{\eta}_r(t) - \sum_{r=1}^{N} GJ\phi_r''(x)\eta_r(t) = 0. \tag{9}$$

Then, multiplying Eq. 9 by $\phi_s(x)$, integrating over the domain from $x = 0$ to $x = L$, and applying the orthonormality conditions presented in Eq. 7 and Eq. 8, one obtains:

$$(1 + I_e\phi_r(x_c)\phi_r(x_c) + I_l\phi_r(x_l)\phi_r(x_l))\ddot{\eta}_r(t) + \omega_r^2\eta_r(t) = 0, \qquad r = 1,2,3,\ldots,N. \tag{10}$$

The attached inertias I_e and I_l affect the shaft's mode shapes and natural frequencies. To include those effects in the analysis, according to Gürgöze (1984) a harmonic solution for $\bar{\eta}_r(t)$ is assumed:

$$\bar{\eta}_r(t) = H_r e^{i\bar{\omega}_r t} \qquad r = 1,2,3,\ldots,N \tag{11}$$

where $\bar{\omega}_r$ is the natural frequency and $\bar{\eta}_r(t)$ is the modal weighting of the uniform shaft with the concentrated inertia. Introducing Eq. 11 into Eq. 10 results in:

$$\omega_r^2 H_r - (1 + I_e\phi_r(x_c)\phi_r(x_c) + I_l\phi_r(x_l)\phi_r(x_l))\bar{\omega}_r^2 H_r = 0. \tag{12}$$

The problem can also be written in matrix form. Thus, introducing the quantities:

$$\begin{aligned}
&\left\{\phi(x)\right\} = \left\{\phi_1(x) \quad \phi_2(x) \quad \ldots \quad \phi_n(x)\right\}^T, \qquad \left\{H\right\} = \left\{H_1 \quad H_2 \quad \ldots \quad H_n\right\}^T, \\
&\left[A\right] = \begin{bmatrix} \omega_1^2 & & & 0 \\ & \omega_2^2 & & \\ & & \ddots & \\ 0 & & & \omega_n^2 \end{bmatrix}, \qquad \left[I\right] = \begin{bmatrix} 1 & & & 0 \\ & 1 & & \\ & & \ddots & \\ 0 & & & 1 \end{bmatrix}, \\
&\left[B'\right] = I_e\left\{\phi(x_c)\right\}\left\{\phi(x_c)\right\}^T + I_l\left\{\phi(x_l)\right\}\left\{\phi(x_l)\right\}^T.
\end{aligned} \tag{13}$$

Eq. 12 can be rewritten as:

$$(\left[A\right] - \left[B\right]\bar{\omega}_r^2)\left\{H\right\}^{(r)} = \left\{0\right\}, \tag{14}$$

where

$$\left[B\right] = \left[I\right] + \left[B'\right]. \tag{15}$$

Note that matrices $\left[A\right]$ and $\left[B\right]$ are symmetric, thus, the eigenvalue problem has real and positive eigenvalues $\bar{\omega}_r$ and eigenvectors $\left\{H\right\}^r$. Then, the r-th mode can be approximated as follows (Gürgöze, 1984):

$$\bar{\phi}_r(x) = \sum_{i=1}^{N} \phi_i(x) H_i^{(r)} \qquad r = 1,2,3,\ldots,N. \tag{16}$$

The electric motor torque and the cylinder's resistive torque can be represented by $f(x,t) = T_m\delta(x-x_m) - T_c\delta(x-x_c)$. The torsional displacement can be obtained by a modal expansion:

$$\theta(x,t) = \sum_{r=1}^{N} \bar{\eta}_r(t)\bar{\phi}_r(x). \tag{17}$$

Introducing Eq. 17 into Eq. 1 the following equation is obtained:

$$\sum_{r=1}^{N} \rho J \bar{\phi}_r(x)\ddot{\bar{\eta}}_r(t) + \sum_{r=1}^{N} I_e\bar{\phi}_r(x)\delta(x-x_c)\ddot{\bar{\eta}}_r(t) + \sum_{r=1}^{N} I_l\bar{\phi}_r(x)\delta(x-x_l)\ddot{\bar{\eta}}_r(t) - \sum_{r=1}^{N} GJ\bar{\phi}_r''(x)\bar{\eta}_r(t) = f(x,t). \tag{18}$$

Imposing the orthonormal conditions below:

$$\int_0^L \rho J\bar{\phi}_r(x)\bar{\phi}_s(x)dx + \bar{\phi}_r(x_c)I_e\bar{\phi}_s(x_c) + \bar{\phi}_r(x_l)I_l\bar{\phi}_s(x_l) = \delta_{rs}, \qquad r,s = 1,2,\ldots \tag{19}$$

$$\int_0^L GJ\bar{\phi}_r''(x)\bar{\phi}_s(x)dx = -\bar{\omega}_r^2\delta_{rs}, \qquad r,s = 1,2,\ldots \tag{20}$$

multiplying Eq. 18 by $\bar{\phi}_s(x)$ and integrating over the domain from $x = 0$ to $x = L$, one obtains the equations of motion in modal coordinates:

$$\ddot{\bar{\eta}}_r(t) + \bar{\omega}_r^2\bar{\eta}_r(t) = q_r(t), \qquad r = 1,2,3,\ldots,N \tag{21}$$

where $q_r(t)$ is:

$$q_r(t) = \int_0^L f(x,t)\bar{\phi}_r(x)dx. \tag{22}$$

Bandgap formation using modal analysis

This section presents the analytical formulation when resonators are attached to the system using modal expansion theory showing the bandgap formation. Two cases are studied, one with identical resonators and the other with a rainbow arrangement. In the first case, all resonators are tuned to the same frequency. In the second case, it is considered different sets of resonators, each set tuned to a different frequency. This latter approach has the goal to produce vibration reduction on a broader bandwidth. The attached crankshaft with evenly distributed resonators is represented in Fig. 2.

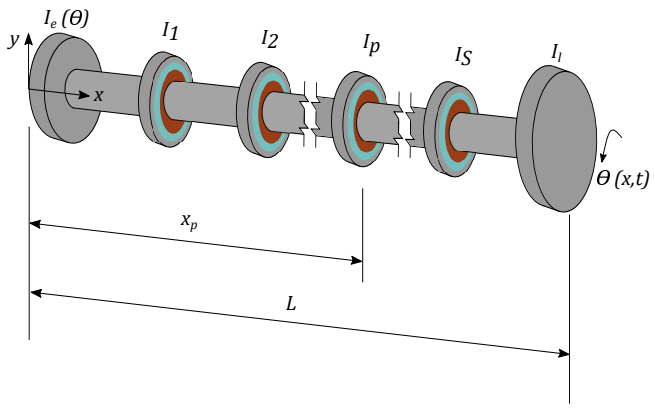

Figure 2 – Crankshaft with resonators.

Identical resonators

Based on the formulation presented in Sugino *et al.* (2017), the equation of motion of the crankshaft, previously presented in Eq. 1, with distributed resonators attached is given by:

$$\rho J\frac{\partial^2\theta(x,t)}{\partial t^2}+I_e\delta(x-x_c)\frac{\partial^2\theta(x,t)}{\partial t^2}+I_l\delta(x-x_l)\frac{\partial^2\theta(x,t)}{\partial t^2}-GJ\frac{\partial^2\theta(x,t)}{\partial x^2}-\sum_{p=1}^{S}k_p\theta_p(t)\delta(x-x_p)=f(x,t) \tag{23}$$

and the equation of motion of each resonator is defined as:

$$I_p\ddot{\theta}_p(t)+k_p\theta_p(t)+I_p\ddot{\theta}(x_p,t)=0, \qquad p=1,2,3,\ldots,S \tag{24}$$

where k_p is the torsional stiffness of the p-th resonator, I_p is the inertia of the p-th resonator, $\theta_p(t)$ is the torsional displacement of the p-th resonator, x_p is the position of the p-th resonator, S is the total number of resonators and $f(x,t)$ is an external torque density.

Assuming that the system is under a concentrated harmonic excitation $f(x,t)=F\delta(x-x_e)e^{i\omega t}$, then employing the modal expansion with N modes as $\theta(x,t)=\sum_{r=1}^{N}\bar{\eta}_r(t)\bar{\phi}_r(x)$ and using the orthonormalization conditions presented in Eqs. 19 and 20, Eqs. 23 and 24 yield to:

$$\ddot{\bar{\eta}}_r(t)+\bar{\omega}_r^2\bar{\eta}_r(t)-\sum_{p=1}^{S}k_p\theta_p(t)\bar{\phi}_r(x_p)=\int_0^L F\bar{\phi}_r(x)\delta(x-x_e)e^{i\omega t}dx, \qquad r=1,2,3,\ldots,N \tag{25}$$

$$-\omega^2 I_p\Theta_p+k_p\Theta_p-\omega^2 I_p\sum_{r=1}^{N}\bar{\phi}_r(x_p)H_r=0. \tag{26}$$

Second to Sugino *et al.* (2017), the steady-state responses $\bar{\eta}_r(t)$ and $\theta_p(t)$ can be described by harmonic functions as $\bar{\eta}_r(t)=H_re^{i\omega t}$ and $\theta_p(t)=\Theta_pe^{i\omega t}$. Inserting the harmonic solutions $\bar{\eta}_r(t)$ and $\theta_p(t)$, and their derivatives, into Eqs. 25 and 26, one obtains respectively:

$$(\bar{\omega}_r^2-\omega^2)H_r-\sum_{p=1}^{S}k_p\Theta_p\bar{\phi}_r(x_p)=F\bar{\phi}_r(x_e) \tag{27}$$

$$\Theta_p=\frac{\omega^2}{\omega_p^2-\omega^2}\sum_{r=1}^{N}H_r\bar{\phi}_r(x_p). \tag{28}$$

Combining Eqs. 28 and 27, the following equation is obtained:

$$(\bar{\omega}_r^2-\omega^2)H_r-\mu\omega^2\sum_{r=1}^{N}\sum_{p=1}^{S}\frac{\omega_p^2}{\omega_p^2-\omega^2}(\rho J+I_e\delta(x-x_c)+I_l\delta(x-x_l))\bar{\phi}_r(x_p)\bar{\phi}_r(x_p)\Delta lH_r=F\bar{\phi}_r(x_e), \tag{29}$$

where $\omega_p^2=k_p/I_p$, $I_p=\mu(\rho J+I_e\delta(x-x_c)+I_l\delta(x-x_l))\Delta l$ and μ is a constant inertia ratio. By assuming identical resonators, one obtains:

$$(\bar{\omega}_r^2-\omega^2)H_r-\mu\omega^2\sum_{r=1}^{N}\frac{\omega_p^2}{\omega_p^2-\omega^2}\left(\sum_{p=1}^{S}(\rho J+I_e\delta(x-x_c)+I_l\delta(x-x_l))\bar{\phi}_r(x_p)\bar{\phi}_r(x_p)\Delta l\right)H_r=F\bar{\phi}_r(x_e), \tag{30}$$

and for a large number of resonators, the following approximation is considered (Sugino *et al.*, 2017):

$$\lim_{S\to\infty}\sum_{p=1}^{S}(\rho J+I_e\delta(x-x_c)+I_l\delta(x-x_l))\bar{\phi}_r(x_p)\bar{\phi}_r(x_p)\Delta l\approx\int_0^L\rho J\bar{\phi}_r(x)\bar{\phi}_r(x)dx+\bar{\phi}_r(x_c)I_e\bar{\phi}_r(x_c)+\bar{\phi}_r(x_l)I_l\bar{\phi}_r(x_l)=1. \tag{31}$$

Thus, Eq. 30 is simplified to:

$$H_r = \frac{F\bar{\phi}_r(x_e)}{(\bar{\omega}_r^2 - \omega^2) - \mu\omega^2\left(\frac{\omega_p^2}{\omega_p^2-\omega^2}\right)}. \tag{32}$$

As addressed by Sugino *et al.* (2017), for identical resonators and a large number of them, the response in the frequency domain, $\alpha_{re}(\omega)$, in physical coordinates is:

$$\alpha_{re}(\omega) = \frac{\Theta(x_r,\omega)}{F(x_e,\omega)} = \sum_{r=1}^{N} \frac{\bar{\phi}_r(x_r)\bar{\phi}_r(x_e)}{\bar{\omega}_r^2 - \omega^2\left(1+\mu\frac{\omega_p^2}{\omega_p^2-\omega^2}\right)}, \tag{33}$$

where x_r is the position where the response is obtained, x_e is the position where the concentrated excitation is applied, ω is the harmonic excitation frequency, $\bar{\omega}_r$ is the natural frequency of the r-th mode, μ is the constant inertia ratio between the total inertia of the resonators and the total inertia of the shaft and ω_p is the natural frequency of the resonators.

Rainbow metastructures

The bandgap formation for rainbow metastructures is similar to the previous case. The core idea is to tune different sets of resonators in different frequencies without adding more inertia to the structure when compared with identical resonators, i.e., μ is constant and equal to the case with identical resonators. To accomplish this, the stiffness of each arrangement of resonators (k_p) is multiplied by a factor ε_n, which follows the profile (Brandão *et al.*, 2022):

$$\varepsilon_n = 1 + 0.1\left(\frac{2n}{S_n} - 1\right), \qquad n = 1,2,3,\ldots,k \tag{34}$$

where S_n is the number of resonators of the n-th set and k is the total number of set of resonators. The factor ε_n generates a variation from -10% to +10% in the stiffness of each array of resonators, which yields different tune frequencies responsible for broadband vibration suppression around the target frequency.

Considering a concentrated harmonic excitation $f(x,t) = F\delta(x-x_e)e^{i\omega t}$ as in the previous case, applying the modal expansion as $\theta(x,t) = \sum_{r=1}^{N} \bar{\eta}_r(t)\bar{\phi}_r(x)$ and the orthonormalization conditions (Eqs. 19 and 20) in the Eqs. 23 and 24, one obtains:

$$\ddot{\bar{\eta}}_r(t) + \bar{\omega}_r^2\bar{\eta}_r(t) - \sum_{p=1}^{S}\varepsilon_n k_p\theta_p(t)\bar{\phi}_r(x_p) = \int_0^L F\bar{\phi}_r(x)\delta(x-x_e)e^{i\omega t}dx, \qquad r = 1,2,3,\ldots,N \tag{35}$$

$$-\omega^2 I_p\Theta_p + \varepsilon_n k_p\Theta_p - \omega^2 I_p\sum_{r=1}^{N}\bar{\phi}_r(x_p)H_r = 0. \tag{36}$$

Introducing the harmonic solutions $\bar{\eta}_r(t)$ and $\theta_p(t)$ into Eq. 35, then:

$$(\bar{\omega}_r^2 - \omega^2)H_r - \sum_{p=1}^{S}\varepsilon_n k_p\Theta_p\bar{\phi}_r(x_p) = F\bar{\phi}_r(x_e). \tag{37}$$

Substituting Eq. 28 into Eq. 37:

$$(\bar{\omega}_r^2 - \omega^2)H_r - \mu\omega^2\sum_{r=1}^{N}\sum_{p=1}^{S}\frac{\omega_p^2}{\omega_p^2-\omega^2}(\rho J + I_e\delta(x-x_c) + I_l\delta(x-x_l))\bar{\phi}_r(x_p)\bar{\phi}_r(x_p)\Delta l H_r = F\bar{\phi}_r(x_e), \tag{38}$$

where $\omega_p^2 = \varepsilon_n k_p/I_p$, $I_p = \mu(\rho J + I_e\delta(x-x_c) + I_l\delta(x-x_l))\Delta l$, μ is a constant inertia ratio.

According to El-Borgi *et al.* (2020), the rainbow metastructure is arranged in k periodic cells that present an array of resonators tuned in different target frequencies, which can form K number of bandgaps. Each cell presents S_k resonators tuned in the resonant frequency ω_k, therefore, the Eq. 38 can be rewritten in this form:

$$(\bar{\omega}_r^2-\omega^2)H_r-\mu\omega^2\sum_{r=1}^{N}\left(\frac{\omega_1^2}{\omega_1^2-\omega^2}\sum_{p=1}^{S_1}(\rho J+I_e\delta(x-x_c)+I_l\delta(x-x_l))\bar{\phi}_r(x_p)\bar{\phi}_r(x_p)+\frac{\omega_2^2}{\omega_2^2-\omega^2}\sum_{q=1}^{S_2}(\rho J+I_e\delta(x-x_c)+\right.$$
$$\left.I_l\delta(x-x_l))\bar{\phi}_r(x_q)\bar{\phi}_r(x_q)+\cdots+\frac{\omega_k^2}{\omega_k^2-\omega^2}\sum_{k=1}^{S_k}(\rho J+I_e\delta(x-x_c)+I_l\delta(x-x_l))\bar{\phi}_r(x_k)\bar{\phi}_r(x_k)\right)\Delta l H_r=F\bar{\phi}_r(x_e), \tag{39}$$

where S is:

$$S=S_1+S_2+\cdots+S_k. \tag{40}$$

Assuming that each set of resonators has a sufficiently large number of periodic cells and that the resonators are evenly well distributed, the following approximation can be considered (El-Borgi *et al.*, 2020):

$$\lim_{S_n\to\infty}\sum_{n=1}^{S_n}(\rho J+I_e\delta(x-x_c)+I_l\delta(x-x_l))\bar{\phi}_r(x_n)\bar{\phi}_r(x_n)\Delta l\approx\int_0^L\rho J\bar{\phi}_r(x)\bar{\phi}_r(x)dx+\bar{\phi}_r(x_c)I_e\bar{\phi}_r(x_c)+\bar{\phi}_r(x_l)I_l\bar{\phi}_r(x_l)=1, \tag{41}$$

with $n=1,2,3,\ldots,k$.

This Riemann sum approximation simplifies Eq. 39 as follows:

$$(\bar{\omega}_r^2-\omega^2)H_r-\mu\omega^2\sum_{n=1}^{k}\frac{\omega_n^2}{\omega_n^2-\omega^2}H_r=F\bar{\phi}_r(x_e), \tag{42}$$

and leads to:

$$H_r=\frac{F\bar{\phi}_r(x_e)}{(\bar{\omega}_r^2-\omega^2)-\mu\omega^2\left(\sum_{n=1}^{k}\frac{\omega_n^2}{\omega_n^2-\omega^2}\right)}. \tag{43}$$

As showed by El-Borgi *et al.* (2020), for a sufficiently large number of periodic cells with a set of k rainbow resonators and evenly well distributed along the structure, the frequency response function, $\alpha_{re}(\omega)$, is given by:

$$\alpha_{re}(\omega)=\frac{\Theta(x_r,\omega)}{F(x_e,\omega)}=\sum_{r=1}^{N}\frac{\bar{\phi}_r(x_r)\bar{\phi}_r(x_e)}{\bar{\omega}_r^2-\omega^2\left(1+\mu\sum_{n=1}^{k}\frac{\omega_n^2}{\omega_n^2-\omega^2}\right)}. \tag{44}$$

RESULTS AND DISCUSSION

This section presents results obtained considering the system's response in the steady state under harmonic excitation, with the goal of identifying the critical zones, associated with higher vibration amplitudes, as well as evaluating the performance of the metastructure in vibration reduction. Two cases are analyzed, in the first, all the resonators are assumed to be identical, with the same inertia, I_p, and the same torsional stiffness k_p. In the second case, a rainbow arrangement is considered with sets of resonators, each set associated with one tuned frequency. In both cases, it is worth mentioning that the added inertia is the same. Table 1 presents system's parameters used in numerical simulations.

Table 1 – System parameters.

Length of the shaft, L	1 m
Diameter of the shaft, d	0.06 m
Elasticity's modulus of the shaft, E	221 GPa
Density of the shaft, ρ	7800 kg/m^3
Poisson's ratio of the shaft, ν	0.3
Inertia of the load, I_l	0.165 kg.m^2
Equivalent inertia of the cylinder, I_e	0.250 kg.m^2
Inertia of p-th resonator, I_p	0.012747 kg.m^2
Number of modes in modal expansion, N	10
Number of attached resonators, S	10

At first, the case with identical resonators is of concern. Figure 3a shows the shaft's response in the frequency domain to a concentrated harmonic excitation with $N = 10$, thus, the first 10 natural modes are considered in the modal expansion. In the figure, the continuous blue line represents the system's response without resonators, while the continuous orange line represents the shaft's response with the attached resonators. The shaded area represents the estimated linear locally resonant bandgap for finite and continuous metastructures as addressed by Sugino *et al.* (2016, 2017):

$$\omega_i < \omega < \omega_i \sqrt{1+\mu} \tag{45}$$

where ω_i is the lower limit of the bandgap and μ is the inertia ratio given by:

$$\mu = \frac{\sum_{p=1}^{S} I_p}{\rho JL + I_e + I_l} = \frac{I_p S}{\rho JL + I_e + I_l}. \tag{46}$$

It is considered that the inertia ratio is $\mu = 0.3$ and the resonators are tuned in $\omega_i = 4000$ Hz so that the bandgap is centralized in the target frequency $\omega_t = 4281$ Hz related to the fourth resonance peak. Figure 3b shows an enlargement in the region of the linear bandgap formation produced by the resonators according to Eq. 45. Usually, the vibration attenuation bandgap range can be increased by adding more resonators (i.e. raising the value of μ), however, there is a saturation point where adding more resonators will not make the bandgap larger.

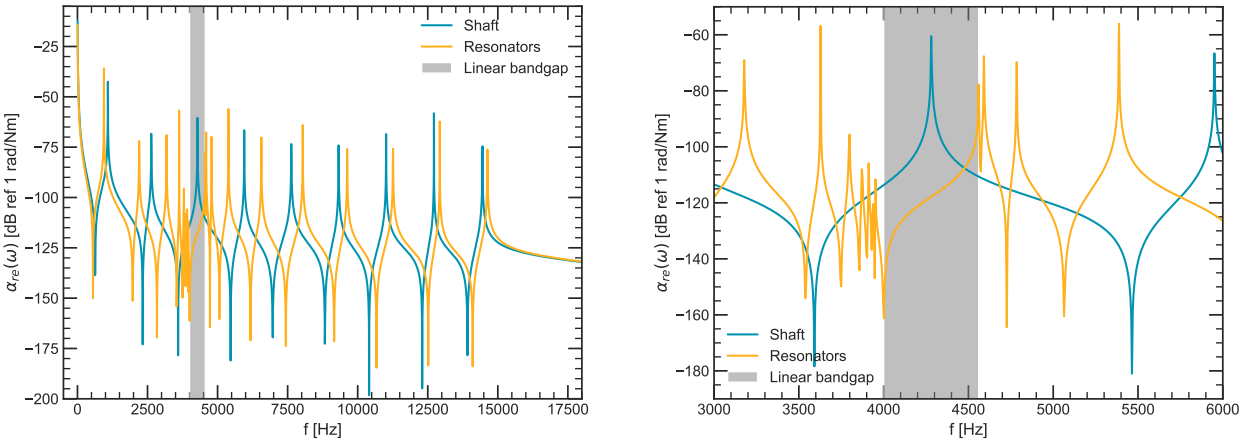

Figure 3 – Frequency response function with identical resonators: (a) frequency response and (b) bandgap area.

Figure 4 shows the dispersion curve when identical resonators are added to the system. The continuous blue line represents the torsional wavenumber (k_T) and the shaded area is the linear bandgap formation. The curve presents discontinuity around $\omega_i = 4000$ Hz, the resonator tuning frequency. In this frequency, propagating waves are suppressed by the resonators creating an attenuation band until $\omega_i = 4560$ Hz. This result is coherent with bandgap limits defined by Eq. 45 and with the frequency response shown in Fig. 3.

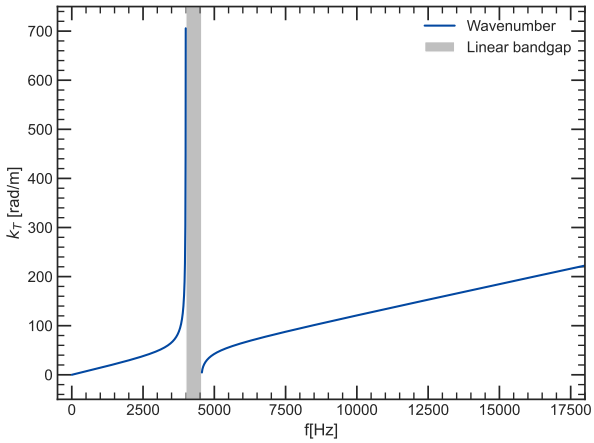

Figure 4 – Torsional wavenumber for the crankshaft with identical resonators

In recent works by Beli *et al.* (2019), Meng *et al.* (2020), Xia *et al.* (2020), El-Borgi *et al.* (2020), and Brandão *et al.* (2022), the use of rainbow metastructures and phononic crystals has been successfully used to increase the vibration attenuation bandwidth using lightweight structures. To enlarge the bandgap, ten sets with 10 resonators each are attached to the shaft, every set with a different tuned frequency, consisting of a rainbow arrangement, and the same added inertia of the previous case ($\mu = 0.3$). Figure 5a presents two curves, the continuous blue line represents the steady state system response without rainbow metamaterials, and the continuous orange line is the response when the rainbow resonators are added. Figure 5b presents an enlargement in the bandgap region, showing that the rainbow metastructure produces a bandgap seven times bigger than identical resonators. This effect happens because each set of resonators follows a specific profile to change the target frequency. On the other hand, the use of rainbow arrangements can not be applied in some cases that require compact designs due to space restrictions.

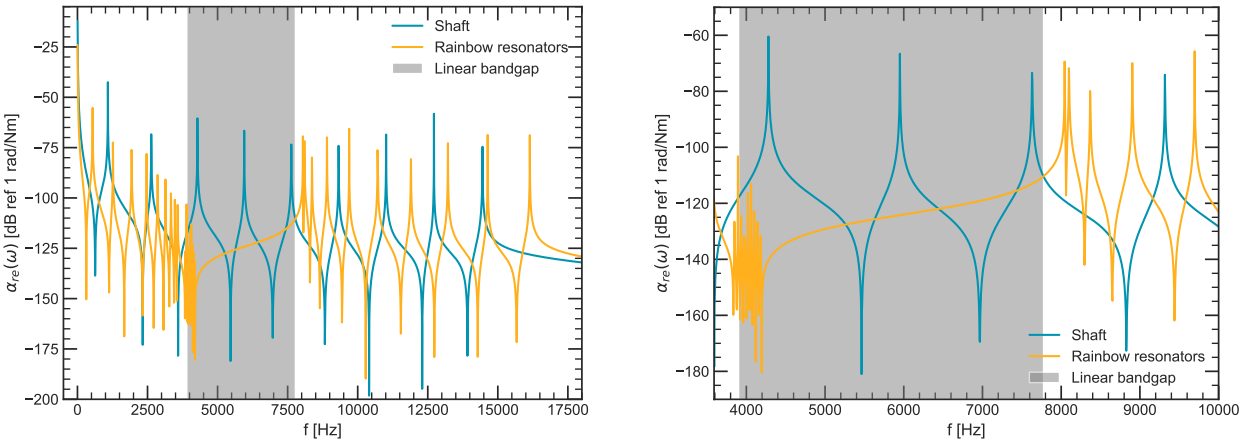

Figure 5 – Frequency response function with rainbow metastructures: (a) frequency response and (b) bandgap area.

CONCLUSIONS

This work investigates the torsional vibration reduction of a reciprocating compressor crankshaft. A continuous model represented the shaft with concentrated inertia elements and harmonic excitation. The mode shapes and natural frequencies were obtained from modal expansion theory. Two different configurations of the metastructure were considered. In the first, identical resonators were attached to the shaft, and in the second, a rainbow arrangement was considered with sets of resonators, each array associated with one target frequency. Results showed that identical resonators successfully attenuated vibration amplitudes in the neighborhood of the target frequency. Moreover, the analysis shows that rainbow metastructures can increase the bandgap seven times without adding more inertia to the system, which is a limiting point for enhancing the bandgap in the case of identical resonators.

ACKNOWLEDGMENTS

The authors are grateful to the Brazilian National Council of Research (CNPq - Brazil), processes number 310850/2019-3 and 433730/2018-8, to CAPES and FAPDF for their support.

REFERENCES

Beli, D., Fabro, A.T., Ruzzene, M. and Arruda, J.R.F., 2019. "Wave attenuation and trapping in 3d printed cantilever-in-mass metamaterials with spatially correlated variability". *Scientific Reports*, Vol. 9, No. 5617.

Brandão, A.A., de Paula, A.S. and Fabro, A.T., 2022. "Rainbow gyroscopic disk metastructures for broadband vibration attenuation in rotors". *Journal of Sound and Vibration*, Vol. 532, No. 116982.

Brusa, E., Delprete, C. and Genta, G., 1997. "Torsional vibration of crankshafts: effects of non-constant moments of inertia". *Journal of Sound and Vibration*, Vol. 205, No. 2, pp. 135–150.

Casalotti, A., El-Borgi, S. and Lacarbonara, W., 2018. "Metamaterial beam with embedded nonlinear vibration absorbers". *International Journal of Non-Linear Mechanics*, Vol. 98, pp. 32–42.

Corbo, M.A. and Melanoski, S.B., 1996. "Practical design against torsional vibration." In *Proceedings of the 25th Turbomachinery Symposium*. Texas A&M University, Turbomachinery Laboratories, Dallas, pp. 189–222.

El-Borgi, S., Fernandes, R., Rajendran, P., Yazbeck, R., Boyd, J. and Lagoudas, D., 2020. "Multiple bandgap formation in a locally resonant linear metamaterial beam: theory and experiments". *Journal of Sound and Vibration*, Vol. 488, No. 115647.

Gürgöze, M., 1984. "A note on the vibrations of restrained beams and rods with point masses". *Journal of Sound and Vibration*, Vol. 96, No. 4, pp. 461–468.

Hu, G., Tang, L., Banerjee, A. and Das, R., 2017. "Metastructure with piezoelectric element for simultaneous vibration suppression and energy harvesting". *ASME Journal of Vibration and Acoustics*, Vol. 139, No. 1.

Huang, Y., Yang, S., Zhang, F., Zhao, C., Ling, Q. and Wang, H., 2012. "Non-linear torsional vibration characteristics of an internal combustion engine crankshaft assembly". *Chinese Journal of Mechanical Engineering*, Vol. 25, No. 4, pp. 797–808.

Kani, M., Khadem, S., Pashaei, M. and Dardel, M., 2016. "Vibration control of a nonlinear beam with a nonlinear energy sink". *Nonlinear Dynamics*, Vol. 83, No. 1-22.

Krödel, S., Thomé, N. and Daraio, C., 2015. "Wide band-gap seismic metastructures". *Extreme Mechanics Letters*, Vol. 4, pp. 111–117.

Liu, Z., Zhang, X., Mao, Y., Zhu, Y., Yang, Z., Chan, C.T. and Sheng, P., 2000. "Locally resonant sonic materials". *Science*, Vol. 289, No. 5485, pp. 1734–1736.

Meirovitch, L., 1997. *Principles and techniques of vibrations*, Vol. 1. Prentice Hall, New Jersey.

Meng, H., Bailey, N., Chen, Y., Wang, L., Ciampa, F., Fabro, A., Chronopoulos, D. and Elmadih, W., 2020. "3d rainbow phononic crystals for extended vibration attenuation bands". *Scientific Reports*, Vol. 10, No. 18989.

Metallidis, P. and Natsiavas, S., 2003. "Linear and nonlinear dynamics of reciprocating engines". *International Journal of Non-Linear Mechanics*, Vol. 38, No. 5, pp. 723–738.

Pasricha, M. and Carnegie, W., 1976. "Effects of variable inertia on the damped torsional vibrations of diesel engine systems". *Journal of Sound and Vibration*, Vol. 46, No. 3, pp. 339–345.

Pasricha, M. and Carnegie, W., 1979. "Formulation of the equations of dynamic motion including the effects of variable inertia on the torsional vibrations in reciprocating engines, part i". *Journal of Sound and Vibration*, Vol. 66, No. 2, pp. 181–186.

Sheng, P., Zhang, X., Liu, Z. and Chan, C.T., 2003. "Locally resonant sonic materials". *Physica B: Condensed Matter*, Vol. 338, No. 1-4, pp. 201–205.

Sugino, C., Leadenham, S., Ruzzene, M. and Erturk, A., 2016. "On the mechanism of bandgap formation in locally resonant finite elastic metamaterials". *Journal of Applied Physics*, Vol. 120, No. 134501.

Sugino, C., Xia, Y., Leadenham, S., Ruzzene, M. and Erturk, A., 2017. "A general theory for bandgap estimation in locally resonant metastructures". *Journal of Sound and Vibration*, Vol. 406, pp. 104–123.

Wachel, J. and Tison, J., 1994. "Vibrations in reciprocating machinery and piping systems". In *Proceedings of the 23rd Turbomachinery Symposium*. Texas A&M University. Turbomachinery Laboratories, Dallas, pp. 243–272.

Xia, Y., Ruzzene, M. and Erturk, A., 2020. "Bistable attachments for wideband nonlinear vibration attenuation in a metamaterial beam". *Nonlinear Dynamics*, Vol. 102, pp. 1285–1296.

RESPONSIBILITY NOTICE

The authors are the only ones responsible for the printed material included in this paper.